IOP Conf. Series: Materials Science and Engineering **61** (2014) 012043 doi:10.1088/1757-899X/61/1/012043

Effect of shape of elastic beam hair on its adhesion with wavy surfaces

Pasomphone Hemthavy[1], Takehiko Yazaki[1], Boqing Wang[1], Yu Sekiguchi[2] and Kunio Takahashi[1]

1 Department of International Development Engineering, Tokyo Institute of Technology, 2-12-1 O-okayama, Meguro-ku, Tokyo 152-8552, JAPAN

2 Precision and Intelligence Laboratory, Tokyo Institute of Technology, 4259-R2-31 Nagatsuta, Midori-ku, Yokohama 226-8503, JAPAN

E-mail: pasomphone@ide.titech.ac.jp

Abstract. An analysis on a tapered elastic beam whose side surface partially adhered to a rigid surface was carried out to study the effect of the beam shape on the gripping force. Considering the total energy of the system, the relation between the gripping force and the displacement was obtained analytically in closed form. The analytical result is significant because it provides an intuitive picture of the gripping force. Although, an individually tapered beam can generate less gripping force for flat or slightly wavy surfaces, compared to a rectangular beam, the analysis result suggests that the tapered beam has more ability to absorb surface waviness. This result can be applied to a multi-beam structure.

1. Introduction

Geckos have a myriad of hierarchical hair structures on their foot fingers, consisting of setae and spatulae. The mechanism of adhesion of the gecko's foot hair was observed to be mainly due to intermolecular surfaces forces [1, 2]. Nano-scaled spatulae at the top of the setae generate an adhesion force so that geckos can hang from roof surfaces as well as climb vertical walls [3]. Though a single foot hair demonstrates a negligible adhesion force, the myriad of slant hair structures enables adhesion to smooth surfaces with high interfacial shear strength [2, 4]. The gecko's foot hair was observed to have a tapered shape towards its tip with a patch on the tip of each spatula [1]. Since these discoveries, many attempts have been made to replicate the functional structures of gecko's foot hair by utilizing polymers of a precise size [5-10]. Multi-beam structures with mushroom tip shapes or tapered beams have also been fabricated and studied experimentally [5, 10]. However, theoretical study on the functional structure of the gecko's foot hair has not been as extensive. Takahashi et al. have researched a release mechanism that allows geckos to take quick steps and their ability to grip rough surfaces from the macroscopic point of view by assuming the seta as a curved slant beam, which can be controlled by normal and tangent forces [3]. Sekiguchi et al. have investigated the adhesive force between a side surface of a rectangular elastic beam and a flat surface of a rigid body [11]. However, the effects of the beam shape have not been clearly studied. In this study, we assume a tapered elastic beam, i.e., one with bending stiffness tapering along its longitudinal axis, to study the effect of the beam shape on the gripping force. By considering the minimum energy condition of the total energy of the system, the effect of the adhesion phenomenon is included in the process for obtaining the relation

between the gripping force and the displacement of the beam. The ability of a multi-tapered beam structure to absorb surface waviness is also discussed.

2. Adhesion model between elastic tapered beam and flat rigid surface

Figure 1 shows a schematic illustration of the elastic tapered beam used in this paper for modeling the function of a single gecko foot hair. The shape of this tapered beam can be expressed by assuming the varying bending stiffness along the longitudinal axis of the beam as

$$EI = E_0 I_0 \left(1 - \frac{x}{L}\right)^n \qquad (0 \le n < 1), \tag{1}$$

where E is the Young's modulus and I is the moment of inertia of the area of the elastic beam, E_0I_0 is the bending stiffness at the base of the beam, L is the length, and x represents the distance along the longitudinal axis of the beam. The width W of the beam is supposed to be constant in order to study the one-directional function of the beam. Figure 2 shows the distribution of the bending stiffness along the longitudinal axis of the beam, plotted by equation (1).

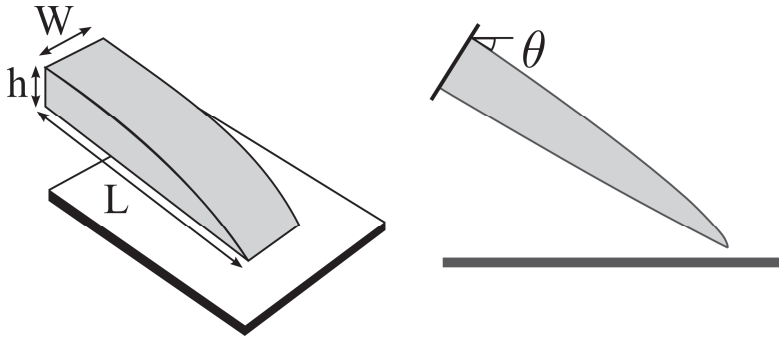

Figure 1. Schematic illustration of a tapered beam model used. The figure on the left-hand side shows the entire view of the beam with its geometries. The figure on the right-hand side is the side view of the beam.

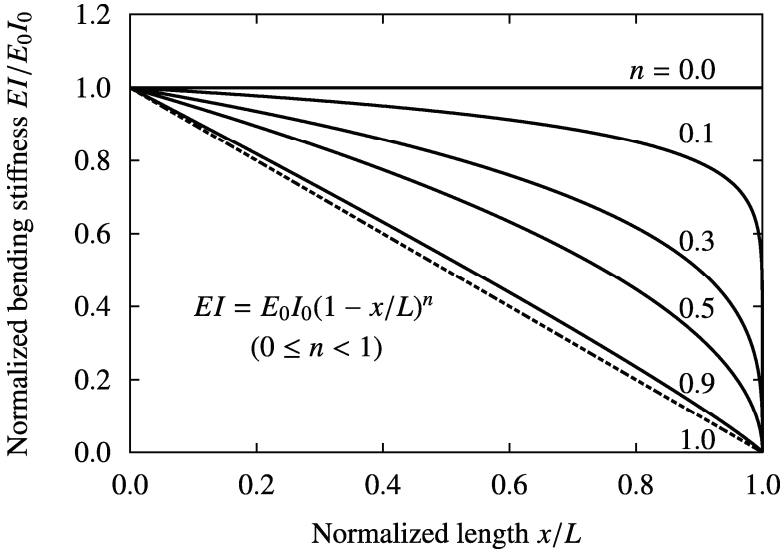

Figure 2. Distribution of the bending stiffness over the distance on the longitudinal axis of the beam.

As shown in figure 2, when n=0 the bending stiffness has a contant value (horizontal straight line), which is equivalent to a rectangular beam, for example. When n=1, the bending stiffness varies linearly along the longitudinal axis toward one end of the beam (dashed line). However, for n=1, there are singularities in the analytic result (described in section 3) which complicate the calculation of the gripping force. Consequently, without losing the essence of the study, we take the range of n to be $0 \le n < 1$.

Figure 3 illustrates the loading and unloading process of the cantilever tapered beam to enable it to grip and release a flat rigid surface. As shown in the figure, the beam is fixed at the base with an inclined angle θ to the horizontal line. The loading process is performed by applying the displacement to the base of the beam, which brings it into contact with the rigid surface, as shown in figure 3(a). When the beam reaches the rigid surface, it starts contacting the surface from its tip edge, which is here defined as "line contact," as shown in figure 3(b). When further displacement is continually applied, the rigid surface presses the edge of the beam with a force f, giving rise to its deformation. As a consequence, the beam adheres to the rigid surface on its bottom side, which is defined as "area contact," as shown in figure 3(c). In static contact, the adhered area of this area contact will settle at an equilibrium that depends on the magnitude of the given displacement.

In the unloading process, starting from area contact, the beam is gradually moved up by applying a displacement in the opposite direction to that of the loading process; this decreases the adhered area, as shown in figure 3(d). When the adhered area finally decreases to line contact, as shown in figure 3(e), the beam finally detaches from the rigid surface, as shown in figure 3(f). This is considered the separation condition of the beam.

In this paper, we adopt the following assumptions for the adhesion model so that the linear beam theory can be applied. The beam is assumed to have small lateral deformation without longitudinal deformation. In addition, the weight and rotation of the beam and the frictional slip between the beam and rigid surface are assumed to be negligibly small.

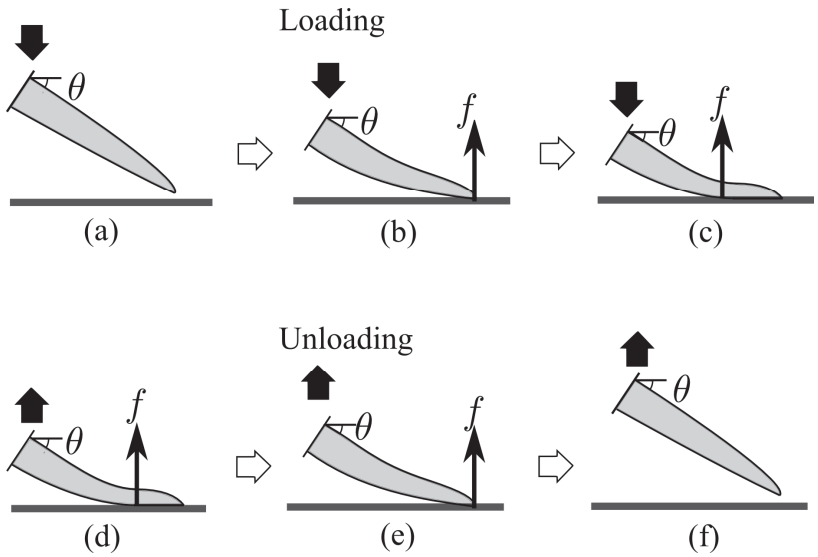

Figure 3. Schematic illustration of the loading process (a)-(c) and unloading process (d)-(f) of the beam. The beam approaches the rigid surface by the applied displacement (a); it starts contacting the surface at its tip edge (line contact) (b); a part of its bottom side adheres to the surface (area contact) (c). Unloading the beam decreases the contact area (d); the contact changes from area contact to line contact (e); the beam finally detaches from the surface (f).

3. Force between the elastic beam and the rigid surface

Our main task here is to obtain the relation between the gripping force of the beam to the rigid surface and the applied displacement. A mathematical model of the beam for line contact and for area contact are assumed, as shown in figures 4 and 5, respectively. A system of coordinate axes (x,y) with the origin located on the longitudinal axis at the fixed end of the beam is used. The displacement d applied to the beam is measured from the rigid surface to the base of the beam with a negative upward direction. When the beam is in contact with the rigid surface, the force f between the rigid surface and the beam acts perpendicularly to the rigid surface.

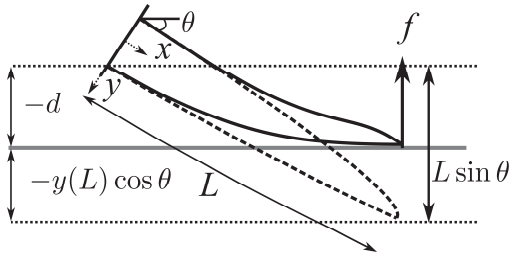

Figure 4. Schematic illustration of line contact of the beam with the rigid surface.

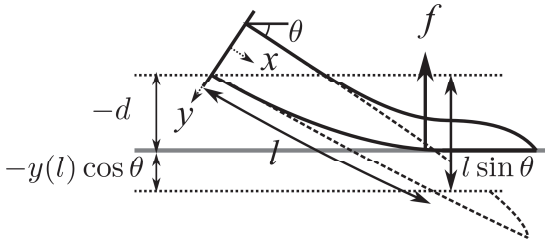

Figure 5. Schematic illustration of area contact of the beam with the rigid surface.

3.1. Force during line contact

During line contact, as shown in figure 4, the force f acting on the tip of the beam causes the beam to deflect slightly. The corresponding deflection of the beam, i.e., $y(x)$, is required to obtain the relation between the force f and the applied displacement d. On the other hand, according to the assumption that the base of the beam is fixed, the boundary conditions $y(0)=0$ and $\mathrm{d}y(x)/\mathrm{d}x=0$ at $x=0$ should be satisfied. From figure 4, the shearing force at any section of the beam, which is given as

$$S = -f\cos\theta \qquad (0 \le x \le L), \tag{2}$$

gives rise to the internal bending moment $M(x)$ of the beam, which is expressed as

$$M(x) = -f\cos\theta(L-x) \qquad (0 \le x \le L). \tag{3}$$

The basic equation of the deflection curve of the elastic beam is given as

$$\frac{d^2y}{dx^2} = -\frac{M(x)}{EI}. \tag{4}$$

From the bending stiffness of the beam, the internal bending moment, and the basic equation of the deflection curve (equations (1), (3), and (4), respectively), the deflection $y(x)$ of the beam, which satisfies the above-mentioned conditions, is obtained as

$$y(x) = -\frac{fL^3\cos\theta}{(n-2)(n-3)E_0I_0}\left\{\left(1-\frac{x}{L}\right)^{3-n} - (n-3)\frac{x}{L} - 1\right\}. \tag{5}$$

From the geometry of the beam shown in figure 4, and the deflection of the beam's tip, i.e., $y(L)$, it yields the relation between the displacement and the deflection of the beam as

$$L\sin\theta = -d - y(L)\cos\theta. \tag{6}$$

Finally, by substituting equation (5) into equation (6), we can obtain the relation between the force f and the applied displacement d for line contact as

$$\tilde{f}\frac{\cos\theta}{\tan\theta} = \frac{(3-n)}{12}\left(\frac{\tilde{d}}{\sin\theta}+1\right), \tag{7}$$

where $\tilde{f}$ *and* $\tilde{d}$ are dimensionless quantities, normalized as $\tilde{f} = f/(12E_0I_0/L^2)$ and $\tilde{d} = d/L$, respectively.

If further displacement is applied to the base of the beam, the beam's tip deflects. Therefore, when the beam deflects so that the slope of the tip equals that of the rigid surface, satisfying the following condition

$$\left.\frac{dy}{dx}\right|_{x=L} = -\tan\theta, \tag{8}$$

the bottom side of the beam begins to adhere to the rigid surface. This is area contact, as shown in figure 5. From equations (5) and (8), the shifting condition from line contact to area contact is obtained as

$$\frac{\tilde{d}}{\sin\theta} = \frac{1}{n-3}. \tag{9}$$

3.2. Force during area contact

The relation between the force *f* and the applied displacement *d* for area contact can be obtained in the same manner as described in the previous subsection, except for the following considerations. During area contact, the adhered portion of the beam conforms to the rigid surface, so that it can be considered the fixed end. Therefore, the force *f* acting on the edge of the adhered portion causes the rest of the beam to deflect, as shown in figure 5. The area of the adhered portion is defined as $(L-l)\times W$, where *l* is the length of the portion of the beam that is not adhered to the rigid surface.

Both ends of the beam are fixed, in contrast to line contact, so the bending moment of the beam is given as

$$M(x) = -f\cos\theta\, x + M_l \qquad (0 \le x \le l), \tag{10}$$

where M_l is determined by the boundary condition of the slope of the beam at *x=l*. The shearing force and the boundary conditions at *x*=0 are the same as those for line contact. The relation between the force and the displacement of the beam for area contact is obtained as

$$\tilde{f}\frac{\cos\theta}{\tan\theta} = \frac{(n-1)(n-2)^2(n-3)}{12} - [(1-\tilde{l})^{1-n}-1]\left\{\frac{\tilde{d}}{\sin\theta} + \frac{(1-\tilde{l})^{1-n}[(n-1)\tilde{l}-1]+1}{(n-2)[(1-\tilde{l})^{1-n}-1]}\right\} \times \frac{}{n(n-2)(n-3)\tilde{l}^2(1-\tilde{l})^{1-n} + (n-3)[(1-\tilde{l})^{2-n}-1]^2 - 2(n-2)[(1-\tilde{l})^{1-n}-1][(1-\tilde{l})^{3-n}-1]}, \tag{11}$$

where $\tilde{l}$ is the normalized non-adhesion length of the beam, defined as $\tilde{l} = l/L$.

However, $\tilde{l}$ is still unknown. In order to determine $\tilde{l}$, it is necessary to take into account the minimum energy condition of the total energy of the system. We define the total energy of the system U_{total} as the sum of the elastic energy U_{elastic} and the surface energy U_{surface}, denoted as

$$U_{\text{total}} = U_{\text{elastic}} + U_{\text{surface}}. \tag{12}$$

The elastic energy due to the deflection of the beam is given as

$$U_{\text{elastic}} = \int_0^l \frac{M^2}{2EI}dx, \tag{13}$$

and the surface energy of the adhered area is

$$U_{\text{surface}} = -\Delta\gamma\times(L-l)\times W, \tag{14}$$

where $\Delta\gamma$ is the work of adhesion required to separate a unit area of adhered surfaces.

The total energy of the system is obtained as

$$\widetilde{U}_{\text{total}} = 12\tan^2\theta\left(\widetilde{f}\frac{\cos\theta}{\tan\theta}\right)^2\left\{\frac{[(1-\widetilde{l})^{2-n}-1]^2-(n-2)^2\widetilde{l}^{\,2}(1-\widetilde{l})^{1-n}}{(n-2)^2(n-3)[(1-\widetilde{l})^{1-n}-1]}\right\}$$
$$+\frac{\tan^2\theta}{12}\frac{n-1}{(1-\widetilde{l})^{1-n}-1}-\Delta\widetilde{\gamma}(1-\widetilde{l})\widetilde{W}, \tag{15}$$

where $\widetilde{U}_{\text{total}} = U_{\text{total}}/(6E_0I_0/L)$ and $\Delta\widetilde{\gamma} = 3\Delta\gamma W/(6E_0I_0/L^2)$. According to the total energy obtained above, $\widetilde{l}$ can be determined by searching for the minimum energy, which occurs when

$$\frac{\partial\widetilde{U}_{\text{total}}}{\partial\widetilde{l}} = 0. \tag{16}$$

4. Calculated results

For convenience in the calculation, we define here the adhesion parameter related to the work of adhesion and the width of the beam as

$$\frac{\Gamma}{\tan\theta} = \frac{\sqrt{3\Delta\widetilde{\gamma}\widetilde{W}}}{\tan\theta}.$$

Solving equation (16) gives us the value of $\widetilde{l}$ for each adhesion parameter. Then, by substituting the value of $\widetilde{l}$ into equation (11), we consequently obtain the relation between the normalized force and the normalized displacement, as shown in figures 6 and 7.

As shown in figure 6, when the beam approaches the rigid surface, the tip of the beam starts touching the rigid surface at P_0, i.e., when $d/(L\sin\theta) > -1$, and the force for line contact expressed by equation (7) will have a positive value. When further displacement is applied between P_0 and P_1, the

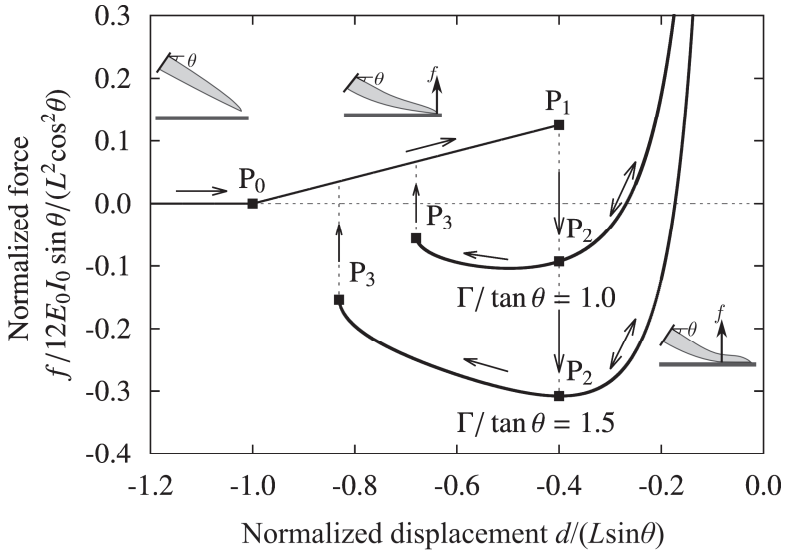

Figure 6. Relation between the normalized force and the normalized displacement, calculated for the adhesion parameter $\Gamma/\tan\theta = 1.0$ and 1.5, and n=0.5.

beam remains in line contact, and the force, which satisfies equation (7), varies along the straight line. The force during line contact is repulsive. After the displacement reaches P_1, which is the shifting condition from line contact to area contact expressed by equation (9), the contact changes to area contact and the force no longer satisfies equation (7). In consequence, the force jumps from P_1 to P_2 to follow equation (11) instead. During area contact, the force curve has several paths according to the value of the adhesion parameter, and the force is attractive. The force varies along each curve, responding to the applied displacement. If an appropriate displacement is applied for the adhesion parameter, the minimum energy exists, and the beam will adhere to the rigid surface at equilibrium. When the beam is unloaded, the force varies along the curve to the left of P_2. When the given displacement reaches the condition $\tilde{l}=1$ at P_3, the beam finally detaches from the rigid surface. The maximum gripping force of the beam can be considered as the measurement of the minimum of each force curve.

Figure 7 shows the relation between the normalized force and the normalized displacement, which is plotted for different values of n. When n=0, i.e., the beam is uniformly rectangular, the analysis result of the present study exactly coincides with the result of the previous work of Sekiguchi [11].

According to the shifting condition from line contact to area contact, expressed by equation (9), the displacement is in inverse proportion to n. This implies that as the value of n increases, the displacement necessary for shifting to area contact decreases. In other words, the tapered beam could have more ability to absorb the surface roughness compared to a uniformly rectangular beam. However, the maximum gripping force generated by an individual tapered beam decreases as the value of n increases.

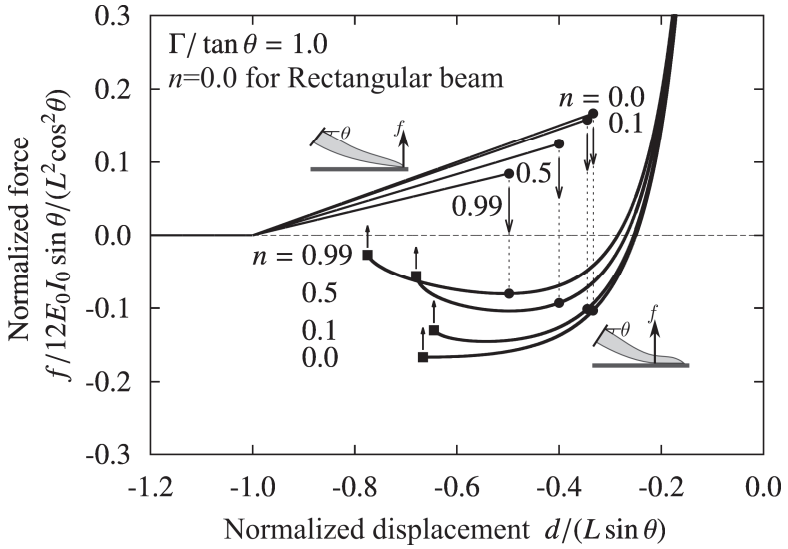

Figure 7. Relation between the normalized force and the normalized displacement for different values of n.

5. Effect of the shape on the gripping force of a multi-beam structure adhering to a wavy surface

To discuss the effect of the beam shape on the gripping force of a multi-beam structure adhering to a wavy surface, we assume a one-dimensional multi-beam structure consisting of a number of individual beams (100 beams were used in this study) fixed to a substrate with a uniform interval and declined angle θ, as shown in figure 8. The waviness of a rigid surface is assumed to be sinusoidal of single wavelength λ and amplitude A. In order to apply the adhesion model of this study, it is assumed that each area on the sinusoidal surface to which the beam's tip adheres is considerably in parallel to the substrate of the multi-beam structure, as shown in figure 9. The multi-beam structure is loaded until its

substrate touches the convex part of the surface, before unloading to measure the gripping force. The total gripping force of the multi-beam structure is considered as the superposition of each individual beam.

Figure 10 shows the analysis result of the normalized gripping force against the normalized amplitude of the surface waviness. The white rectangular mark denotes the results of the multi-rectangular beam structure, and the black triangle mark denotes the results of the tapered beam structure. As shown in the figure, the multi-rectangular beam structure can generate a larger gripping force compared to the multi-tapered beam structure when the rigid surface is flat or slightly wavy.

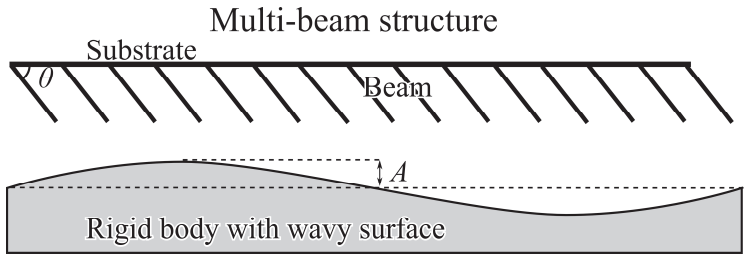

Figure 8. Schematic illustration of a one-dimensional multi-beam structure contacting to a sinusoidal wavy surface.

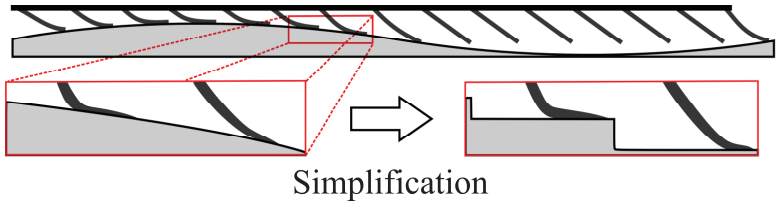

Figure 9. Simplification of the sinusoidal surface as steps parallel to the substrate to measure the gripping force.

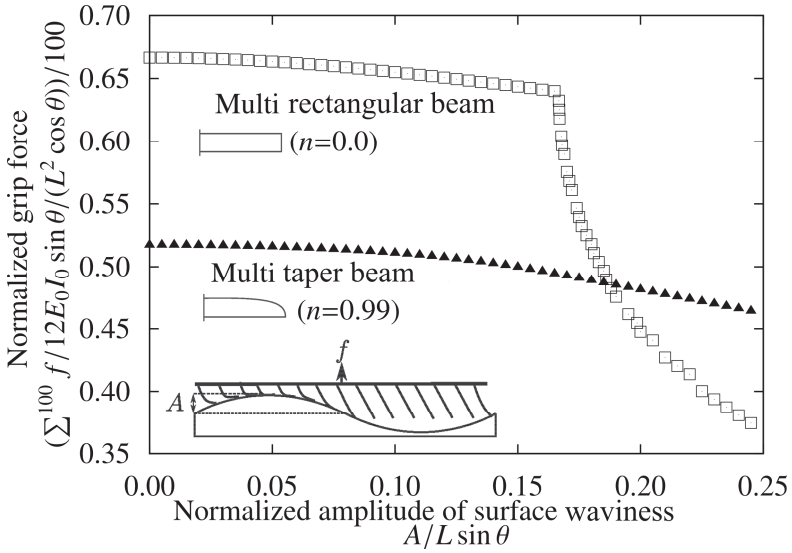

Figure 10. Normalized gripping force of a one-dimensional multi-beam structure against normalized amplitude of surface waviness.

However, when the normalized amplitude $A/(L\sin\theta)$ of the surface waviness exceeds a certain value, e.g., 0.16 for this analysis, its gripping force rapidly decreases and becomes lower than that of the multi-tapered beam structure. The analysis result suggests that the multi-tapered beam structure could have more ability to absorb the surface waviness compared to the multi-rectangular beam structure.

6. Conclusion

A tapered beam model with a varying bending stiffness along its longitudinal axis was assumed to study the relation between the gripping force and the applied displacement analytically. The analysis results were obtained in closed form, which provides an intuitive picture of the gripping force. Although each tapered beam can generate less gripping force than a rectangular beam, increasing the value of *n* can enable the tapered beam to absorb surface waviness. When the beams are compiled to form a multi-beam structure, rectangular beams create a greater gripping force for flat or slightly wavy surfaces, whereas tapered beams create a greater gripping force for more wavier surfaces. The result of this study is considered significant for designing a grip-and-release device using tapered beams.

References

[1] Autumn k, Liang Y A, Hsieh S T, Zesch W, et al. 2000 *Nature* **405** 681
[2] Autumn K, Sitti M, Liang Y A, Peattie A M, Hasen W R, Sponberg S, Kenny T W, Fearing R, Israelachvili J N and Full R J 2002 *PNAS* **99**(19) 12252
[3] Takahashi K, Berengueres J O L, Obata K J and Saito S 2006 *International Journal of Adhesion and Adhesives* **26** 639
[4] Murphy M P, Aksak B and Sitti M 2009 *Small* **5**(2) 170
[5] Sitti M and Fearing R S 2002 *IEEE-NANO* 137
[6] Aksak B, Murphy M P and Sitti M 2007 *Langmuir* **23** 3322
[7] Murphy M P, Kim S and Sitti M 2009 *Applied Materials & Interfaces* **1**(4) 849
[8] Kim S, Sitti M, Xie T and Xiao X 2009 *Soft Matter* **4** 3689
[9] Yu J, Chary S, Das S, Tamelier J, Turner K L and Israelachivili J N 2012 *Langnuir* **28** 11527
[10] Asbeck A, Dastoor S, Parness A, Fullerton L, Esparza N, Soto D, Heyneman B and Cutkosky M 2009 *IEEE International Conference on Robotics and Automation* 2675-80
[11] Sekiguchi Y, Hemthavy P, Saito S and Takahashi K 2012 J. Adhesion Sci. Technol. 26 23 2615